Research Article | Vol. 28, No. 21 / 12 October 2020 / Optics Express 30513
Optics EXPRESS

Three-dimensional real-time darkfield imaging through Fourier lightfield microscopy

GABRIELE SCROFANI,* GENARO SAAVEDRA, MANUEL MARTÍNEZ-CORRAL, AND EMILIO SÁNCHEZ-ORTIGA

3D Imaging and Display Laboratory, University of Valencia, Dr. Moliner 50, 46100 Burjassot, Spain
emilio.sanchez@uv.es

Abstract: We report a protocol that takes advantage of the Fourier lightfield microscopy concept for providing 3D darkfield images of volumetric samples in a single-shot. This microscope takes advantage of the Fourier lightfield configuration, in which a lens array is placed at the Fourier plane of the microscope objective, providing a direct multiplexing of the spatio-angular information of the sample. Using the proper illumination beam, the system collects the light scattered by the sample while the background light is blocked out. This produces a set of orthographic perspective images with shifted spatial-frequency components that can be recombined to produce a 3D darkfield image. Applying the adequate reconstruction algorithm high-contrast darkfield optical sections are calculated in real time. The presented method is applied for fast volumetric reconstructions of unstained 3D samples.

1. Introduction

Darkfield (DF) microscopy is a well-established technique which provides an image of the light scattered by the specimen, blocking out the unscattered light. This technique produces a high-contrast image of the sample details on a dark background, without the need for staining or for special preparation of the specimen [1–4]. The implementation of DF only requires an illumination beam with a radially oblique distribution, in such a way that the light scattered by the sample is collected by the microscope objective (MO) whilst the illumination beam is blocked out by the aperture stop (AS). Due to its ease-of-use and straightforward implementation, DF is a powerful tool for the inspection and monitoring of different bacteria [1–2] as well as for the analysis and characterization of different unstained biological specimens, such as microtubules [3], red-blood cells [4].

In this manuscript, we combine the benefits of DF with Fourier lightfield microscopy (originally named as Fourier integral Microscopy – FiMic) [5,6]. FiMic represents a variation of the standard lightfield microscopes (LMic) [7,8] in which a microlens array located at the image plane performs a sampling of the spatio-angular content of optical rays emitted by the sample. Lightfield microscopy has been shown as a powerful technique for fast recording and reconstruction of 3D volumes [9–10]. On the contrary, in FiMic a lenslet array (not necessarily microlenses) is located at the (AS), or at a conjugated plane of it, allowing the direct capture of a set of different orthographic perspective images (named here as elemental images) of the sample. The main advantages of FiMic over LMic realizations are: (a) The elemental images (EI) are captured directly, without any need of additional processing; (b) Each EI covers a large field of view, then, at the region of interest the system is linear and shift invariant (LSI), this permits to define a single PSF for the whole specimen making possible the easy application of deconvolution procedures [11]; (c) The conflict between the wave-nature of light and the lightfield concept is avoided, then both the lateral resolution and the depth of field are largely increased.

Different approaches can be applied to refocus axial planes of the sample [12–14], to obtain optical sections [15,16] or even to display the 3D sample in a multi-perspective monitor [17].

#404961 https://doi.org/10.1364/OE.404961
Journal © 2020 Received 12 Aug 2020; revised 2 Sep 2020; accepted 2 Sep 2020; published 28 Sep 2020

Optics EXPRESS

The FiMic optical configuration is especially well suited for the implementation of a DF mode, since the lens array is placed at the Fourier plane where the background light can be filtered out from the light scattered by the sample. In what follows, we will use the acronym DFiMic for naming the darkfield Fourier lightfield microscope.

2. Darkfield Fourier lightfield microscope

Starting from the FiMic architecture, there are mainly two ways of implementing the DF mode (see Fig. 1). The first method is based on the use of an illumination ring (see Fig. 1(a)), which projects onto the sample, by means of a condenser lens, a distribution of mutually incoherent plane waves whose propagation vector α_{ill} falls in a cone. Then, the light diffracted by the sample is collected by the AS whereas the undiffracted light is blocked out. Hence, the lens array collects only the light that has been scattered, or diffracted, by the sample. As a consequence, any lens is capturing not only a different perspective of the sample, but also different spatial-frequency content of the scattered light. The EIs can be computationally recombined by using standard lightfield refocusing algorithms in order to obtain DF volumetric reconstructions of the scattered field. The main condition for efficiently performing this method is illuminating with a cone of light of an angle superior to the numerical aperture ($NA = sin\ \alpha$) of the objective. Hence, the NA of the system is limited by the convergence angle of the illumination (NA_{ill}).

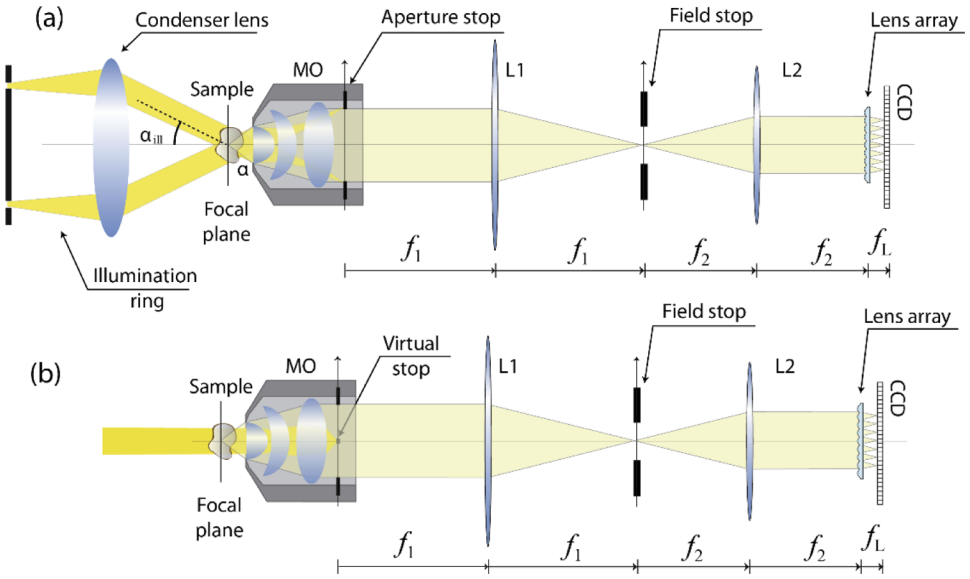

Fig. 1. DFiMic schemes use a relay system, composed by L_1 and L_2, to conjugate the microlenses with the AS, and an adequate illumination beam. (a) Based on the use of an illumination ring; and (2) Base on a plane wave illumination and post-filtering out the central EI.

A second approach is based on the use of a plane wave in such a way that the background light is exclusively collected by the central lens of the array whereas the rest of lenses collect the light scattered by the sample. Considering the central lens as a spatial filter, a DFiMic reconstruction can be achieved by omitting the information captured by it in the reconstruction process. This has been represented in the layout (see Fig. 1(b)) by drawing a virtual stop, which accounts for the removal of the light collected by the central lenslet. In this case there is no limitation regarding the NA of the microscope objective as the unscattered light is filtered out by the lens array. Consequently, this approach provides a better lateral resolution compared to the

Optics EXPRESS

standard method. Although this method is feasible and avoids the limitations due to the numerical aperture of the objective, it has as main drawback because in practical realizations the central lens collects most of the light. Taking into account the limited dynamic range of the detectors, the number of photons collected by the external lenslets is several orders of magnitude smaller than those collected by the central one. Consequently, the effective dynamic range of external EIs is strongly reduced due to the saturation of the central image. This effect could be prevented by manufacturing a lenslet array in which the central lens is blocked with an opaque stop.

Taking into account the easier feasibility of the illumination through the ring and the technical limitations of the second method, this manuscript will be focused on the description and practical implementation of the first approach.

Provided that the DFiMic system captures a collection of high-contrast perspective images, each with different spatial frequency content, and blocks out the background light in a single-shot, the standard reconstruction algorithms can be applied to perform volumetric reconstruction of the scattered light. One possible method is the use of a backpropagation algorithm [13–19], which is based on proper shifts of each EI with respect to the central EI and the normalized summation of the resulting fields. Different refocusing planes are obtained depending on the amount of shift applied to the EIs. A recent algorithm [16] based on the shift and normalized multiplication of the EIs has shown the capability of the FiMic to produce, by computational means, optically-sectioned depth images in case of sparse fluorescent samples. This algorithm, known as shift and multiply (S&M), although designed for its application in fluorescence regime, can be applied successfully in other regimes, provided that the elemental images show, mainly, sparse scatterers over a dark background. This is the case is of DFiMic, which in case of sparse samples, produces a collection of high-contrast images of the specimen with a dark background. It must be mentioned that an alternative approach based on a time-multiplexed capture of images with different illumination angles produces a similar result in terms of a multiperspective collection of DF images from that can be computationally combined to produce multiple refocusing planes [20]. However, that method cannot work in real time or with dynamic scenes.

It is important to notice that this variation in the illumination mode of the FiMic does not change the optical parameters of the microscope such as lateral resolution (ρ) or depth of field (DOF). In particular, the lateral resolution limit of the DFiMic is the same as the FiMic, which is given by [6]

$$\rho_{\mathrm{DFiMic}} = \frac{\lambda}{2\,NA} K$$

being K the number of EIs in the corresponding transverse dimension and λ the illumination wavelength.

3. Experimental verification

In order to show the feasibility of a DFiMic, a prototype was built using the following components: a tunable illumination ring that combined with the condenser lens produces a cone of light with a convergence angle (NA_{ill}) ranging from 0.1 to 0.25, a microscope objective (4× NA=0.2 Nikon), an optical relay of lateral magnification $M = -0.375$ composed by two achromatic doublet lenses of focal lengths $f_1 = 200\ mm$ and $f_2 = 75\ mm$ (Edmund Optics), a lens array consisting of a set of lenses with focal length $f = 7.94$ mm and radius equal to 1 mm (APH-Q-P1000-R3.63 manufactured by AMUS), and a CCD camera (Imaging source DFM 370UX250-ML) with 2448×2048 pixels of 3.45 µm of size. With this setup, and according to the formulae reported in [6] it is possible the capture of EIs with resolution limit $\rho_{FiMic} = 12\ \mu m$.

As stated before, DF requires an illumination beam such that $NA < NA_{ill}$. Otherwise, the unscattered light is not blocked out. In a preliminary experiment a high-resolution negative USAF 1951 test target was used as sample. In Fig. 2 we show the elemental images captured with the DFiMic, but adjusting the illumination to two cases: (a) $NA > NA_{ill}$=0.1 and (b) $NA < NA_{ill}$=0.25.

Optics EXPRESS

In the first case, Fig. 2(a), the projected ring is slightly smaller than the AS. Note that only the lenseslets illuminated by the ring provide perceivable images. The inner elemental images are so dark that cannot be used for the post processing. On the contrary, in the second case (Fig. 2(b)) the projected ring is slightly larger than the AS. Naturally, this image is darker, but all the elemental images are sufficiently illuminated and store the expected perspective and spatial-frequency information.

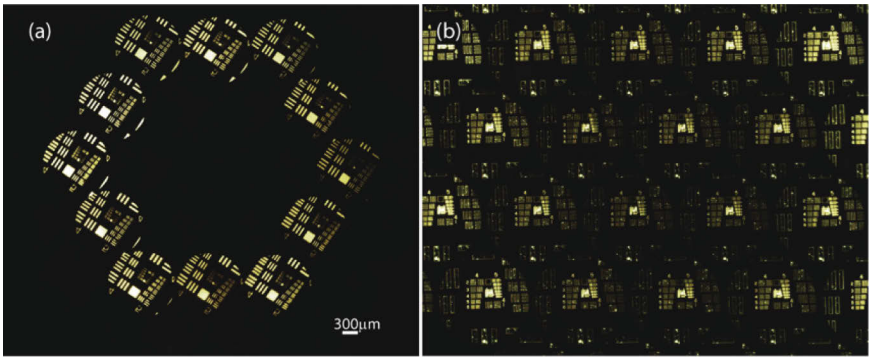

Fig. 2. DFiMic images captured by using an illumination ring of divergence angle: (a) Smaller than the numerical aperture of the microscope objective ($NA > NAill$); and (b) Higher than the numerical aperture of the microscope objective, ($NA < NAill$).

Next, we used Fig. 2(b) as the input for two different reconstruction algorithms: the standard shift and sum (S&S) and the recently reported S&M. These algorithms permit the calculation of refocused images in a number of planes perpendicular to the optical axis (and, naturally, parallel to the USAF). In this case the sample is two-dimensional. Thus, the most important plane is the one that contains the object, shown in Fig. 3. Both algorithms performed equally well in terms of the lateral resolution: the last group of the test to be resolved is the 5-1 (marked with a red box in Fig. 3), determined from the contrast of the profiles in Fig. 3(c). This group which corresponds to a resolution limit of 15 μm. Note that this value is close to the lateral resolution predicted by theory (12 μm). As expected, in the (y, z) meridian sections shown in Fig. 3, the S&M shows better optical sectioning capability.

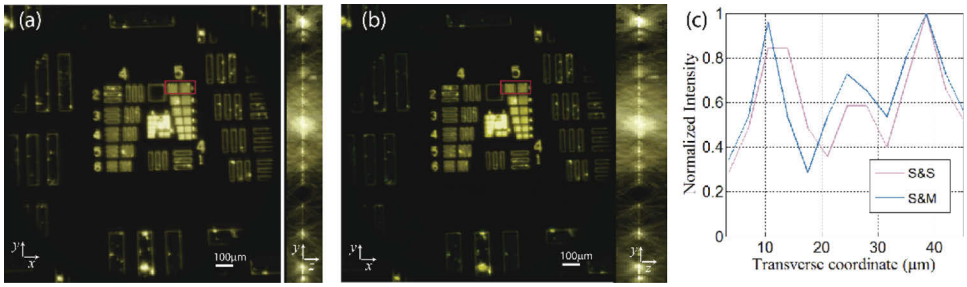

Fig. 3. In-focus plane and axial cut of the 3D stack obtained for DFiMic images by means of (a) S&S algorithms and (b) S&M algorithm. (c) Profiles of the 5-1 group (marked with a red box in (a) and (b)) of the USAF test for both algorithms.

Once verified the feasibility of DFiMic, we performed a second experiment aiming to show the capability of capturing 3D images of transparent sparse samples. We used a sample consisting of soap bubbles floating in water. A DFiMic image obtained with the prototype is shown in Fig. 4(a). Clearly, the EIs are appropriate for the application of the S&M algorithms as the bubbles are

Optics EXPRESS

sparsely distributed over the volume, the scattering is produced in their outer surface, and the background is dark.

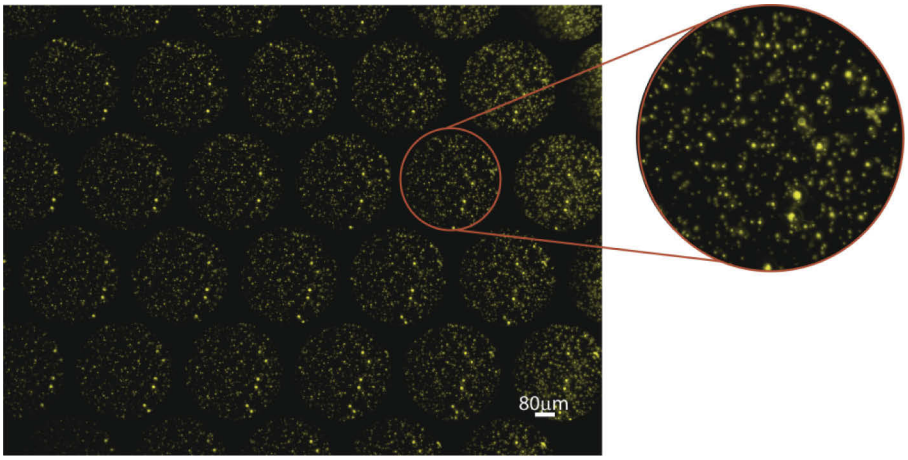

Fig. 4. EIs images of bubbles floating in water obtained with the DFiMic. In the inset we show the enlarged copy of one of the EIs.

Using those EIs as the input for the S&M algorithm we calculated the stack of optically-sectioned refocused images. The execution of the full algorithm, which allowed the calculation of 25 z-images took 375 ms. Thus, although in this case we have used a static sample, the DFiMic clearly can be used with dynamic specimen. From the z-stack a rendered 3D volume of 2.3×2.3 mm in the transverse directions and 1.05 mm in the axial one was created, see Fig. 5. It is interesting that the optical-sectioning capability of the proposed protocol permits the immersive observation of this 3D transparent sample.

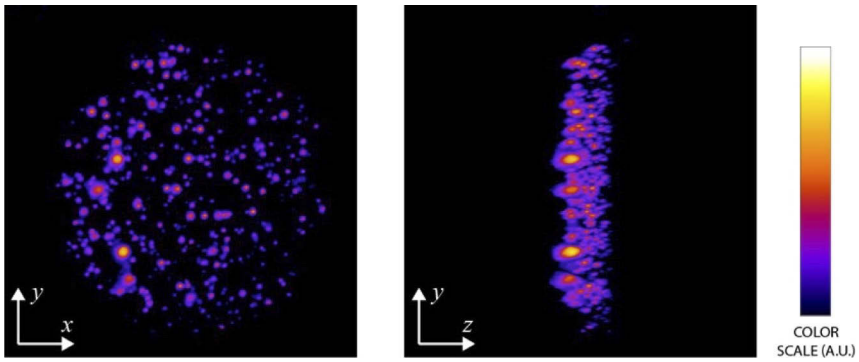

Fig. 5. Two frames of Visualization 1, a rotating movie with the 3D render of the bubbles sample. The color bar represents intensity values in arbitrary units.

Finally, we went a step further and applied the DFiMic for obtaining the 3D image of a bleached zebrafish embryo embedded in agarose as sample. In Fig. 6 we show the EIs. Then we proceeded as in the previous case, and calculated the z-stack. The resulting orthographic views and the 3D reconstruction based on the maximum intensity projection of the z-stack are represented in Fig. 7. Again, the utility of our protocol is apparent, since it permits to capture the 3D structure of the zebrafish in real time after a single shot.

Optics EXPRESS

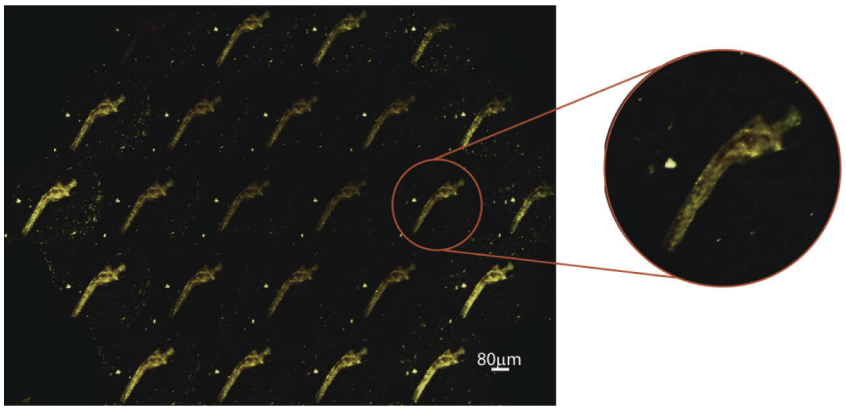

Fig. 6. EIs of a bleached zebrafish embryo captured with the DFiMic.

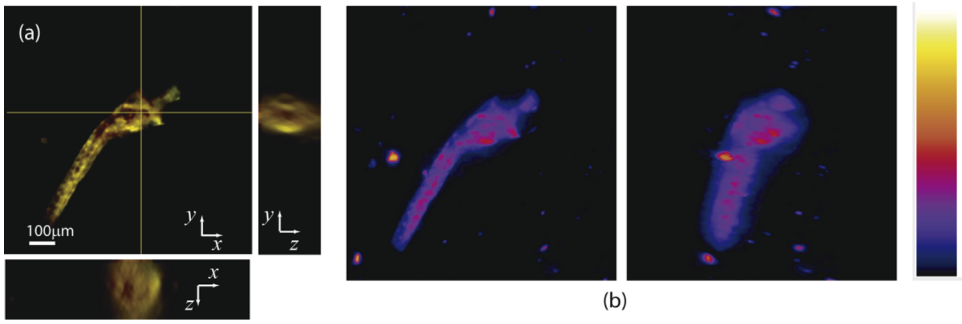

Fig. 7. (a) Orthographic views of the zebrafish extracted from the projection of the z-stack calculated from the EIs (real-color) and (b) Two frames of Visualization 2, a rotating movie with the 3D render of the zebrafish sample. The color bar represents intensity values in arbitrary units.

4. Conclusion

We have demonstrated the application of darkfield imaging to a Fourier lightfield microscope. The system, named here as DFiMic, permits the capture in real time of 3D sparse transparent samples. Interesting features of proposed DFiMic is that it provides optically-sectioned images in real time. Thus, it can be used for imaging static and also dynamic unstained samples. To demonstrate the utility of our proposal, we have performed three experiments in which we have produced single-shot volumetric reconstructions of 3D samples.

Funding

Generalitat Valenciana (PROMETEO/2019/048); Ministerio de Ciencia, Innovación y Universidades (RTI2018-099041-B-I00).

Acknowledgements

The authors acknowledge the help of Jim Swoger from EMBL (Barcelona) for providing the bleached zebrafish embryo.

Optics EXPRESS

Disclosures

The authors declare that there are no conflicts of interest related to this article.

References

1. T. Horio and H. Hotani, "Visualization of the dynamic instability of individual microtubules by dark-field microscopy," Nature **321**(6070), 605–607 (1986).
2. R. M. Macnab, "Examination of bacterial flagellation by dark-field examination of bacterial flagellation by dark-field microscopy," J. Clin. Microbio. **4**, 258–265 (1976).
3. M. M. Singletary, J. J. Crawford, and D. M. Simpson, "Dark-field microscopic monitoring of subgingival bacteria during periodontal therapy," J Periodontol. **53**(11), 671–681 (1982).
4. S. Keegan, J. Arellano, and T. Gruner, "Validating the measurement of red blood cell diameter in fresh capillary blood by darkfield microscopy: A pilot study," Advances in Integrative Medicine **3**(1), 11–14 (2016).
5. A. Llavador, J. Sola-Pikabea, G. Saavedra, B. Javidi, and M. Martinez-Corral, "Resolution improvements in integral microscopy with Fourier plane recording," Opt. Express **24**(18), 20792–20798 (2016).
6. G. Scrofani, J. Sola-Pikabea, A. Llavador, E. Sanchez-Ortiga, J. C. Barreiro, G. Saavedra, J. Garcia-Sucerquia, and M. Martinez-Corral, "FiMic: design for ultimate 3D-integral microscopy of in-vivo biological samples," Biomed. Opt. Express **9**(1), 335–346 (2018).
7. J.-S. Jang and B. Javidi, "Three-dimensional integral imaging of micro-objects," Opt. Lett. **29**(11), 1230–1232 (2004).
8. M. Levoy, R. Ng, A. Adams, M. Footer, and M. Horowitz, "Light field microscopy," ACM Trans. Graph. **25**(3), 924–934 (2006).
9. N. C. Pégard, H. Y. Liu, N. Antipa, M. Gerlock, H. Adesnik, and L. Waller, "Compressive light-field microscopy for 3D neural activity recording," Optica **3**(5), 517–524 (2016).
10. N. Antipa, G. Kuo, R. Heckel, B. Mildenhall, E. Bostan, R. Ng, and L. Waller, "DiffuserCam: lensless single-exposure 3D imaging," Optica **5**(1), 1–9 (2018).
11. A. Stefanoiu, G. Scrofani, G. Saavedra, M. Martinez-Corral, and T. Lasser, "What about super-resolution in fourier lightfield microscopy?" Opt. Express **28**(11), 16554–16568 (2020).
12. J. Arai, F. Okano, H. Hoshino, and I. Yuyama, "Gradient-index lens-array method based on real-time integral photography for three-dimensional images," Appl. Opt. **37**(11), 2034–2045 (1998).
13. M. Cho and B. Javidi, "Computational reconstruction of three-dimensional integral imaging by rearrangement of elemental image pixels," J. Disp. Technol. **5**(2), 61–65 (2009).
14. A. Llavador, E. Sánchez-Ortiga, G. Saavedra, B. Javidi, and M. Martíınez-Corral, "Free-depths reconstruction with synthetic impulse response in integral imaging," Opt. Express **23**(23), 30127–30135 (2015).
15. E. Sánchez-Ortiga, A. Llavador, G. Saavedra, J. García-Sucerquia, and M. Martinez-Corral, "Optical sectioning with a Wiener-like filter in Fourier integral imaging microscopy," Appl. Phys. Lett. **113**(21), 214101 (2018).
16. E. Sanchez-Ortiga, G. Scrofani, G. Saavedra, and M. Martinez-Corral, "Optical sectioning microscopy through single-shot Lightfield protocol," IEEE Access **8**, 14944–14952 (2020).
17. M. Martíınez-Corral and B. Javidi, "Fundamentals of 3D imaging and displays: A tutorial on integral imaging, light-field, and plenoptic systems," Adv. Opt. Photonics **10**(3), 512–566 (2018).
18. H. Arimoto and B. Javidi, "Integral three-dimensional imaging with digital reconstruction," Opt. Lett. **26**(3), 157–159 (2001).
19. S.-H. Hong, J.-S. Jang, and B. Javidi, "Three-dimensional volumetric object reconstruction using computational integral imaging," Opt. Express **12**(3), 483–491 (2004).
20. G. Zheng, C. Kolner, and C. Yang, "Microscopy refocusing and dark-field imaging by using a simple LED array," Opt. Lett. **36**(20), 3987–3991 (2011).